Turkish Journal of Electrical Engineering and Computer Sciences

Volume 26 | Number 6 Article 18

1-1-2018

The measurement of shielding effectiveness for small-in-size ferrite-based flat materials

İSA ARAZ

Turkish Journal of Electrical Engineering & Computer Sciences

http://journals.tubitak.gov.tr/elektrik/

Research Article

Turk J Elec Eng & Comp Sci
(2018) 26: 2996 – 3006

doi:10.3906/elk-1803-162

The measurement of shielding effectiveness for small-in-size ferrite-based flat materials

İsa ARAZ[1*]

[1]Atomic Sensors Laboratory, National Institute of Metrology, TÜBİTAK, Kocaeli, Turkey

Received: 23.03.2018 • **Accepted/Published Online:** 16.07.2018 • **Final Version:** 29.11.2018

Abstract: This work presents the results of our studies on the electromagnetic interference shielding effectiveness of small-in-size samples of ferrite composition microwave absorber prepared by using the ceramic method. The shielding effectiveness measurement was performed using the complex intrinsic parameters of the material. The coaxial holder method with the well-known test technique based on transmission/reflection measurements was used in the experimental setup. Complex intrinsic parameters were measured in the frequency range of 2–18 GHz by using the Nicholson–Ross–Weir (NRW) method with an automated test setup. First, the shielding effectiveness was measured by conventional test method and then it was calculated using complex intrinsic parameters with the NRW method. Comparison was made between measured and calculated SEs. By using a new method the SE was determined as a function of the complex intrinsic parameters of materials ϵ, μ, and frequency. This method is preferred in order to provide higher accuracy in determining material electromagnetic shielding effectiveness for small-in-size materials. For the first time, the shielding effectiveness of small-sized samples has been measured in the frequency range between 2 and 18 GHz by using the NRW method.

Key words: Electromagnetic interference, ceramic technology, coaxial transmission line, complex intrinsic parameters, microwave absorber, shielding effectiveness measurement

1. Introduction

The electromagnetic noise generated by man-made devices has increased over the last few decades. Electromagnetic interference (EMI) is an electromagnetic noise that has adverse effects on public health in addition to malfunctioning of electronic equipment. In order to reduce these effects, many novel materials were synthesized, such as EMI shielding screens, screen coatings, flexible conductor screens, shielding textiles, and broadband microwave absorbers.

Ferrite-based absorbers are one of the most appropriate materials for suppressing EMI due to their complex intrinsic parameters. Designing the composition of EMI shielding materials with the desired level of attenuation is not an easy task, which involves a coaction of complex intrinsic properties (σ, ϵ, and μ) of shielding materials.

The characterization of their electromagnetic properties is intensively studied, as well as the synthesis of absorbers [1–3]. One of the most important parameters to characterize the absorber materials is the shielding effectiveness (SE) parameter. There are several methods for measuring the SE of absorber materials. However, for small samples of only a few centimeters or less than a centimeter in size, test standards and evaluation

*Correspondence: isa.araz@tubitak.gov.tr

procedures are not available. The conventional test standards, MIL-STD-285 [4] and ASTM D4935 [5], were prepared for evaluating the shielding effectiveness of relatively large plane structures. However, these standards cannot be used for nanoengineered and nanoreinforced materials due to their limited operating range and relatively large dimensions required. Several recent studies focused on the development of new methods or alternative measurement devices to characterize the shielding properties of nanoengineered materials in small-sized structures [6, 7]. All these previous studies mainly recommended alternative methods similar to the ASTM D4935 standard by modifying the insertion loss measurement. In those studies, a new sample holder is used each time for different materials and each time validation of the sample holder is required. Additionally, in the ASTM D4935, a coaxial waveguide holder with interrupted inner conductor is also used, which further causes a contact resistance problem. In order to overcome contact resistance, a reference specimen and reference measurements are required [8].

In this study, we recommend using the standard test setup and the standard calibrated test fixture as a sample holder and hence the validation of the sample holder is not required each time. In the proposed method, the inner conductor is not interrupted. Therefore, a reference specimen and reference measurements are not necessary. The main drawback of our test method is the requirement for a sophisticated extraction algorithm, which was prepared according to the Nicholson–Ross–Weir (NRW) method. However, this method is practical and reliable in high-frequency SE measurements for small and flat samples.

In this study, first of all, we measured all S parameters following the ASTM D5568 14 Standard and then extracted complex intrinsic parameters using the measured S parameters of the prepared sample [9]. Then we calculated the SE using the NRW method with complex intrinsic parameters and compared the results with the measurement results obtained similar to the ASTM ES7-83 [10] method. The ASTM ES7-83 Test Method for Electromagnetic Shielding Effectiveness of Planar Materials (Withdrawn 1988) is based on voltage (U1, U2) measurements. U1 is the voltage measured at the output of the sample holder/waveguide without sample material and U2 is the voltage measured at the output of the sample holder/waveguide with sample material. The effectiveness of the shielding parameter of a small sample was measured for the first time using the NRW method. The results are reported for a broad spectrum of frequencies.

2. Shielding effectiveness

The shielding theory is derived from Maxwell's equations. Schelkunoff derived the shielding effectiveness of an infinitely spread thin surface from shielding theory in 1943 [11] and a further study of shielding was carried out by Shulz et al. [12]. The total shielding effectiveness was defined in logarithmic scale and calculated by using the following equation [11–13]:

$$SE_T(dB) = 20log[RL] + 20log[AL] + 20log[MIR]. \tag{1}$$

The multiple path reflection loss (MIR) is usually omitted in the high-frequency band ($\sim$1 GHz or higher). The reflection loss (RL) and the absorption losses (AL) are calculated by using the measured complex scattering parameters, S11 and S21, from the following formulas [11, 14]:

$$RL(dB) = 20log[1 - R], \tag{2}$$

$$AL(dB) = 20log[T/1 - R], \tag{3}$$

$$R = [S11]^2, \tag{4}$$

$$T = [S21]^2. \tag{5}$$

Alternatively, the reflection loss (RL) and the absorption loss (AL) parameters can be obtained precisely by using complex material permeability and permittivity by using the NRW technique. The NRW technique is presented in Section 4.

3. Sample preparation

The Co-doped barium hexaferrite ($BaFe_{11}CoO_{19}$) is chemically composed of $BaCO_3$, Fe_2O_3, and CoO (all at 99.999 % purity). In order to increase the crystal growth at lower temperatures 1% boron (B_2O_3) was added [15]. It was synthesized using conventional mechanical powder processing techniques for ceramic materials. The synthesized powder was pressed to get a 3-mm-thick toroid-shaped pellet. The prepared pellet was sintered at a temperature of 1000° C for 2 h. The results of the characterization of the prepared sample were reported by Araz et al. [16].

4. Measurement and calculation details

The processes for defining the attenuation level of an EMI shield can be complicated depending on the applications. Some of the well-known test methods for shielding performances are shielded room, coaxial transmission line method, open area, and shielded box test [17, 18]. The complex intrinsic parameters of screening materials critically influence the EMI shielding performance. That is why it is so important to calculate them correctly.

The complex intrinsic dielectric permittivity and magnetic permeability have real and imaginary parts. The T/R measurement technique is a well-known method for extracting the complex dielectric permittivity and magnetic permeability. There are several extraction techniques [19, 20]. Determining the extraction method depends on parameters such as the length of the sample, measured S-parameters, conversion speed, and accuracy in results. The NRW method is the commonly used one and it allows the calculation of both the complex permittivity and complex permeability directly from the measured S-parameters.

In this study, first of all, we measured S-parameters, which allowed us to extract the complex intrinsic parameters of the sample by following the ASTM D5568 standard by using the T/R method. In the experimental test setup, we used a standard 7-mm coaxial airline as a sample holder. Then we extracted complex permeability and permittivity from the measured S-parameters. We further precisely determined the reflection loss and absorption loss parameters by using the NRW formulas, instead of directly using the S-parameters. After that, we calculated SE parameters according to Eq. 1. Finally, we measured SE according to the ASTM ES7-83 Standard and compared the result with the result of SE calculated by the NRW method. To extract the complex permeability and permittivity values from the measured S parameters, we developed a MATLAB algorithm using the NRW method. We compared the results of complex intrinsic parameters that were obtained with our program and with commercial software (HP Company, Material Analyzer Software).

4.1. SE measurement with coaxial holder method

Theoretically, SE (dB) can be associated with the insertion loss (IL) of the sample because the sample is placed between the source and signal analyzer. Regarding the ASTM ES7-83 Standard, the vector network analyzer was used to perform SE (dB) and the insertion loss might be explained in terms of the transmission scattering

parameters S21S and S21E, with ('S' stands for sample) and without ('E' stands for empty) the material sample, respectively.

$$SE(dB) = S21E(dB) - S21S(dB) \tag{6}$$

We put the prepared sample tightly inside the coaxial airline waveguide and then performed the S21 parameters by using a vector network analyzer (VNA) in the frequency range of 2–18 GHz. In the beginning, we connected a coaxial airline to the two-port vector network analyzer (HP model 8510-3) and calibrated it. After the calibration, we recorded S21E data without a sample in the air as a reference. Then the toroid-shaped sample was tightly placed inside the coaxial airline (7-mm) waveguide. After that we started the measurement of complex S21S data. The automation measurement used in the test setup can be seen in Figure 1.

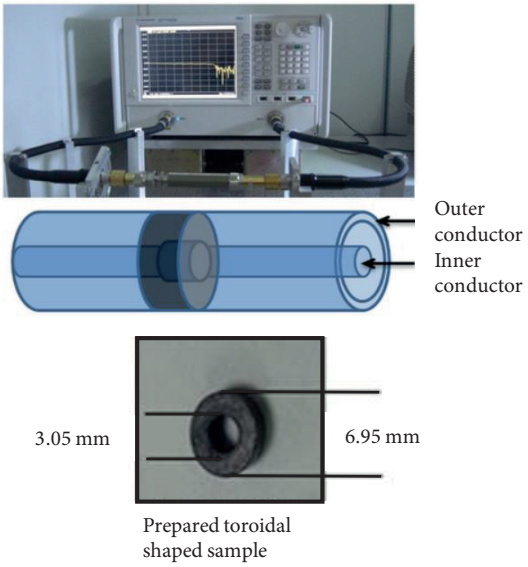

Figure 1. The S parameter measurement test setup for using a two-port VNA (top), a schematic representation of sample inside the sample holder (middle), and picture of prepared sample (bottom).

We used the HP type standard calibration kit (HP 85051-60007, 7 mm, 50 ohm airline) as a coaxial airline in the measurements. Its dimensions are 7 mm outer diameter, 3 mm inner diameter, and 10 mm length. In our case, the dimensions of the sample are 6.95 mm outer diameter, 3.05 mm inner diameter, and 3 mm length. A picture of the synthesized sample and schematic representation of the sample inside the sample holder are seen in Figure 1.

4.2. SE calculation with NRW method

According to the NRW method [21–23], the complex reflection coefficient is defined as:

$$\Gamma = X \pm \sqrt{X^2 - 1}. \tag{7}$$

The appropriate sign is chosen in order to get abs $(\Gamma) \leqslant 1$. In terms of S parameters, X can be written as

$$X = \frac{S11^2 - S21^2 + 1}{2 \times S11}. \tag{8}$$

The complex transmission coefficient is defined by the following equation:

$$P = \frac{(S11 + S21) - \Gamma}{1 - (S11 + S21) \times \Gamma} \tag{9}$$

In order to extract the complex permittivity and permeability of the sample, the measured S values are used. Subsequently, the reflection losses (RLs) are precisely calculated using the following equations [13, 24, 25]:

$$RL = 20 \times log(abs\frac{z-1}{z+1}), \tag{10}$$

where

$$z = z_r/z_0 \tag{11}$$

and

$$Z_r = \sqrt{\frac{\mu_r}{\epsilon_r}} tanh[j(\frac{2 \times pi \times f \times d}{c}) \times \sqrt{\epsilon_r \times \mu_r}. \tag{12}$$

Here, Z_r is impedance of the waveguide with the sample and Z_o is impedance of the empty waveguide (air), and d is the sample length in cm and f is the frequency. The absorption loss (AL) is obtained by using Eq. (3). Finally, total SE is calculated using Eq. (1). The first term of Eq. (1) represents the reflection loss obtained from Eq. (10), and the second term represents the absorption loss obtained from Eq. (3). R and T terms in Eq. (3) were derived as in Eqs. (4) and (5). However, here, S11 and S21 are not used from measured raw data. They are derived in terms of Γ and P based on the NRW formulas as appeared in Eqs. (13)–(15).

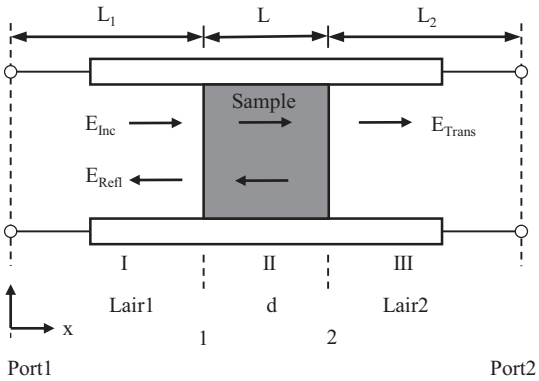

Figure 2. Transmitting of electromagnetic waves through and reflecting from a sample in a transmission line [26].

As shown in Figure 2, it is possible to relate the scattering parameters of the P and Γ coefficients to S_{ij} using the normal ray tracing method or the impedance method.

$$S11 = R_1^2[\frac{\Gamma(1-z^2)}{1-\Gamma^2 Z^2}] \tag{13}$$

$$S21 = R_1 R_2 \frac{Z(1-a^2)}{1-\Gamma^2 Z^2}] \tag{14}$$

Here, Z = e^{-Pd}, R_i = $e^{-P_{air}L_{air1/2}}$ i=1,2, and

$$P_{air} = j\sqrt{\frac{\omega^2\mu_r\epsilon_r}{c^2} - \frac{2\Pi}{\lambda_c}} = j\frac{\omega}{c}. \tag{15}$$

Z is the impedance waveguide with sample, Γ and P are reflection and propagation coefficients, d is the sample thickness in cm, L_{air1} is the air gap length between calibration plane 1 and sample, L_{air1} = D2-D1, and L_{air2} is the length of air between calibration plane 2 and sample, L_{air2} = D4–D3 as seen in Figure 3. P_{air} is the propagation coefficient in the air. Take into account that the cutoff wavelength is approaching infinity (λ_c goes to ∞) in the coaxial airline.

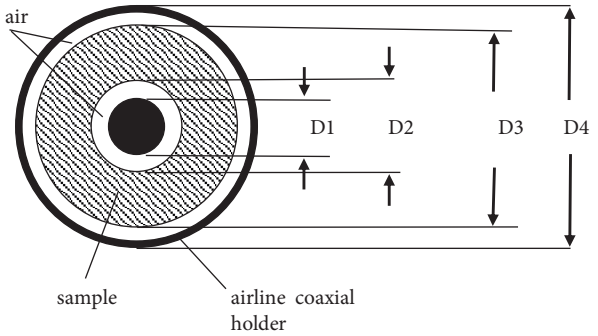

Figure 3. The sample in a coaxial sample holder with an air gap.

A schematic representation of the test sample inside the coaxial test holder is seen in Figure 3. In the case of our studies the dimensions are as follows: D1 = 3 mm, D2 = 3.05 mm, D3 = 6.95, mm and D4 = 7 mm.

5. Results and discussion

The experimental setup, according to the ASTM 5568 Standard, consists of an HP model 8510-3 Vector Network Analyzer (VNA) and a 10-mm-long gold-plated coaxial airline with a precision 7-mm connector. Before starting the measurement, we calibrated the VNA using the two-port measurement method by measuring the reflection and transmission coefficients in the 2–18 GHz frequency range. Then we connected an empty coaxial airline between the input and output ports of the VNA and performed an S-parameters measurement to check for any connector mismatches. After the calibration and verification procedure, we performed an SE measurement using a method similar to the ASTM ES7-83 Standard. First of all, we performed a thorough transmission measurement without a sample inside the coaxial airline to obtain S21 in dB. In the second step, we put the prepared toroidal-shaped sample inside the 7-mm coaxial airline and then S21 data were recorded again in dB units. Finally, we performed four S parameter measurement again in the 2–18 GHz frequency range. We extracted the complex intrinsic permeability and permittivity from the measured S values using both our proprietary MATLAB algorithm based on the NRW method and commercial software. The compared results are shown in Figures 4–7.

First, we measured SE using a conventional test method similar to the ASTM ES7-83 Standard as seen in Figure 8. In the second step, we calculated using the extracted complex intrinsic parameters absorption loss (AL) and reflection loss (RL) as seen in Figures 9 and 10. In the third step, the shielding effectiveness (SE) was calculated as presented in Figure 11 (black line). Finally, we compared the calculated SE with the measured SE as seen in Figure 11.

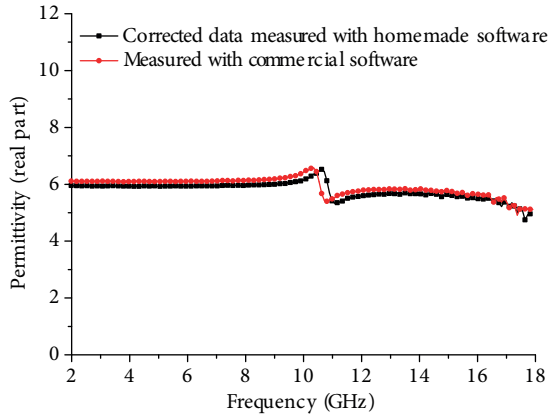

Figure 4. Comparison of results obtained with commercial and our own software for the real part of the permittivity of the sample.

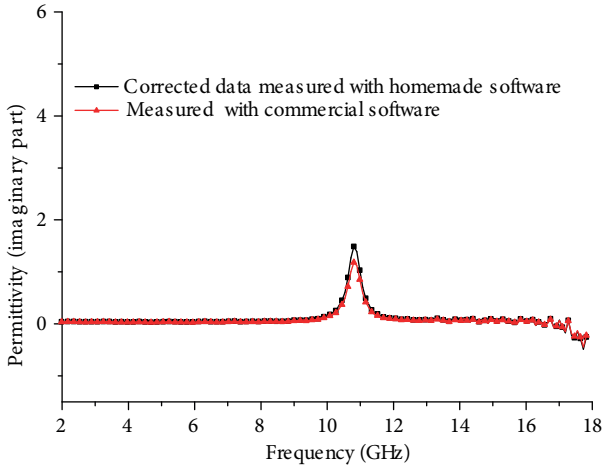

Figure 5. Comparison of results obtained with commercial and our own software for the imaginary part of the permittivity of the sample.

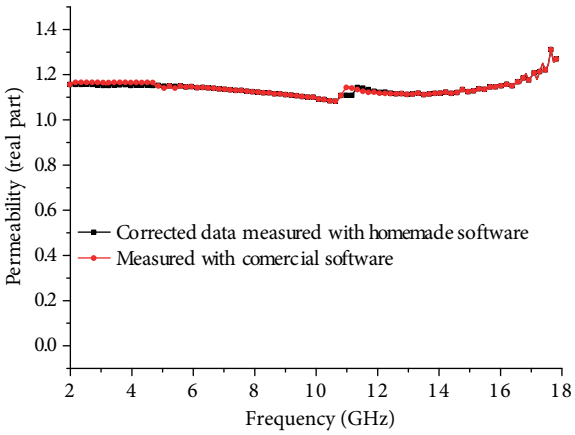

Figure 6. Comparison of results obtained with commercial and our own software for the real part of the permeability of the sample.

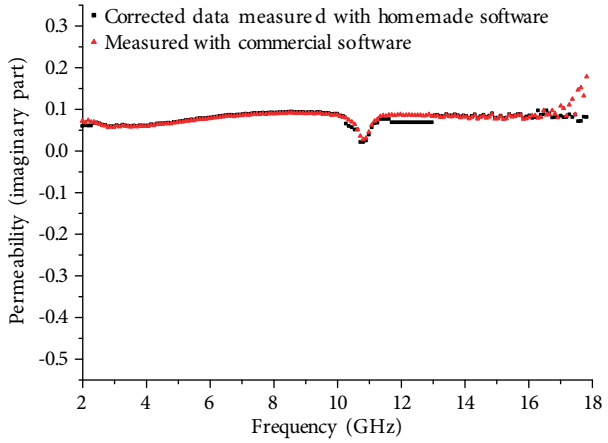

Figure 7. Comparison of results obtained with commercial and our own software for the imaginary part of the permeability of the sample.

The obtained reflection loss results are calculated using the extracted complex intrinsic parameters. They were extracted using our proprietary algorithm and then compared with the result obtained using the commercial material characterization software by HP Company. The extracted complex intrinsic parameters are shown in Figures 4 to 7. The results obtained using our software are almost identical to those of the commercial software. There is only a slight phase shift. We can say that this phase shift comes from the wavefront rotation before and after the sample in the waveguide. Probably there are physical path distance differences between our algorithm and the commercial one. Figure 9 shows the mean value of the absorption loss, which was found to be around –15.9 dB. The average reflection loss obtained is around –19 dB as seen in Figure 10. The results of the reflection loss calculation obtained using both our proprietary algorithm and the commercial one are shown in Figure 10. There is only a slight amplitude difference. We can say that this amplitude difference comes from the phase shift. Additionally, it may also come from the difference in data fitting methods between the commercial algorithm and ours. Considering the extraction results and calculated reflection loss results, our algorithm works quite well compared with the commercial one so the calculated results should be reasonable. All the presented plots

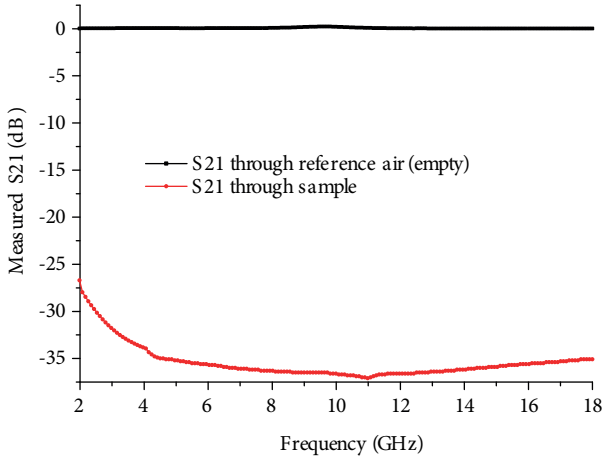

Figure 8. Insertion loss measurement in terms of S21 parameters.

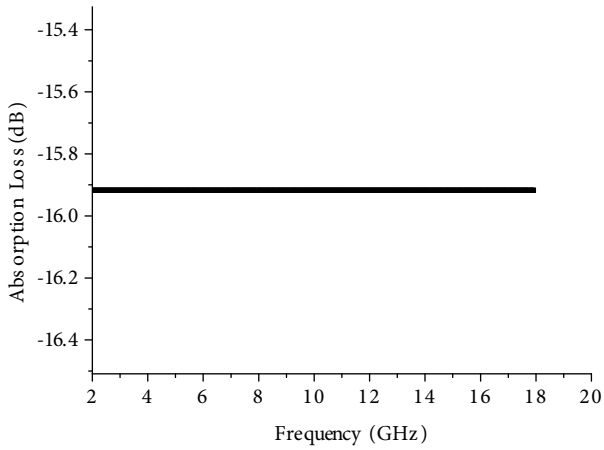

Figure 9. Frequency dependence of the mean value of the absorption loss.

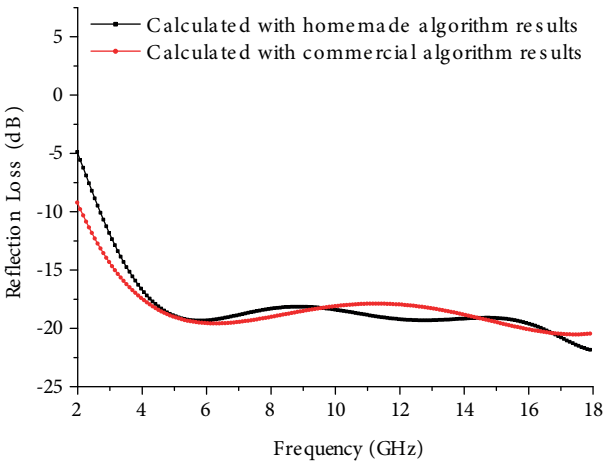

Figure 10. Reflection loss calculated using results of the proprietary algorithm and commercial software results.

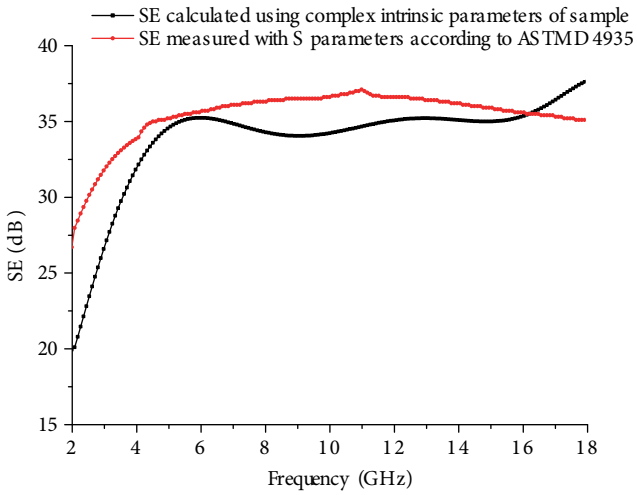

Figure 11. SE measurement according to the definition of SE given in ASTM ES7-83 Standard and SE calculated using intrinsic parameters of the sample with the NRW method.

were obtained using the fitted data. It appears that the impedance mismatch in the connector in the 2–4 GHz frequency range that arises due to the variation is higher in that measurement frequency range. The average reflection loss obtained is around –19 dB and it is almost flat in the 4 to 16 GHz frequency range. At higher frequencies, the reflection loss slightly increases up to –21.5 dB as expected. We can see the same effects on the shielding side. That is the higher difference in the 2–4 GHz frequency range as seen in Figure 11. There is a slight amplitude difference between the calculated and measured SE values. However, the calculated SE and the measured SE exhibit the same behavior, except for in the high-frequency region. Since the resonance region is close to 12 GHz, SE is expected to be flat, except in the resonance region. Moreover, SE represents more or less the same characteristic with the loss mechanism, which is mostly driven by the reflection loss. Calculated shielding effectiveness value was found to be around 35 dB in the resonance region. It is increasing slightly in the higher frequency range, as expected, because of the increased reflection loss at higher frequencies

as seen in Figures 10 and 11. On the other hand, the measured SE value was found to be around 36 dB in the resonance region, decreasing slightly in the higher frequency range, which basically reflects the transmission (S21) characteristics. In the NRW method, we can find the frequency dependence of RL precisely. We can easily determine or estimate the frequency dependence of the SE performance of material from the RL results without normalizing the transmission power. In this respect, we can understand that SE calculated using the NRW method can be accepted as the correct and reliable results for small samples. Besides the reliability of this new SE measurement method, there are also some other advantages. First of all, we can use the standard measurement method and setup to find the complex intrinsic parameters. Second, we can use the standard calibration toolkits as a sample holder such as the coaxial airline and rectangular waveguide with respect to our measurement frequency range. Thus, there is no need to prepare and calibrate sample holders as in the case of the conventional SE test method and similar test methods [1, 4, 5]. On the other hand, the need to prepare the sample to fit tightly in the sample holders and to use the extraction algorithm are the drawbacks of this method. The commercial algorithm is expensive and gives out extracts only of the complex intrinsic parameters.

6. Conclusion

The shielding effectiveness determination was done by measuring complex S parameters using a commercial automated measurement setup. Then, using the measured S parameters, the complex permittivity and complex permeability of the toroid-shaped sample were extracted using a proprietary MATLAB algorithm. For the first time, the reflection loss and absorption loss of the ferrite composition have been calculated using the NRW method and the total shielding effectiveness has been obtained. The calculated shielding effectiveness value is around 35 dB and is almost flat between 4 GHz and 16 GHz.

There are similar studies on electromagnetic properties of barium hexaferrite with different substitutions. La–Co-substituted barium hexaferrite ($Ba_{1-x}La_xCo_xFe_{2-x}O_{19}$ (x = 0.0, 0.1, 0.5, 0.6)) was studied by Srivastava et al. [27]. They found that the maximum reflection loss of 16.5 dB occurs at 17.59 GHz. Additionally, they showed that the real part of the permittivity was around 6 and real part of the permeability was around 1.6 in the 12–18 GHz frequency range. In another similar study, the magnetic and microwave absorbing properties of $BaFe_{12-2x}Co_xZn_xO_{19}$ (x = 0.0; 0.2; 0.4; 0.6) were reported by Handoko et al. [28]. They reported similar values of complex intrinsic parameters of Co- and Zn-doped barium hexaferrite materials. It can be concluded that the numerical data in our study are consistent with the literature on ferrite materials.

The coaxial transmission air line technique with the NRW method is easy and usable for the measurement of shielding effectiveness of thin RF absorber materials in a wide frequency range but is suitable only for small samples.

References

[1] Sarto MS, Tamburrano A. Innovative test method for the shielding effectiveness measurement of conductive thin films in a wide frequency range. IEEE T Electromagn C 2006; 48: 331-340.

[2] Badic M, Marinescu M, Stefan M, Aciu LE, Williams D. An iterative method to calculate absorption loss in conductive dielectrics. In: IEEE International Symposium on Electromagnetic Compatibility; 2006; Portland, OR, USA.

[3] Catrysse JA, Goeije MD, Steenbakkers W, Anaf L. Correlation between shielding effectiveness measurements and alternative methods for the characterization of shielding materials. IEEE T Electromagn C 1993; 35: 440-444.

[4] MIL-STD-285. Military Standard Attenuation Measurements for Enclosures Electromagnetic Shielding, for Electronic Test Purposes. Washington, DC, USA: Government Printing Office, 1956.

[5] ASTM D 4935-99. Standard Test Method for Measuring the Electromagnetic Shielding Effectiveness of Planar Materials. New York, NY, USA: ASTM, 1999.

[6] Vasquez H, Espinoza L, Lozano K. Simple device for electromagnetic interference shielding effectiveness measurement. IEEE T Electromagn C 2009; 220: 62-68.

[7] Tadeusz WW, Janukiewicz JM. Methods for evaluating the shielding effectiveness of textiles. Fibres Text East Eur 2006; 14: 59.

[8] Tamburrano A, Desideri D, Maschio A, Sarto MS. Coaxial waveguide methods for shielding effectiveness measurement of planar materials up to 18 GHz. IEEE T Electromagn C 2014; 56: 102-111.

[9] ASTM ES7–83. Test Method for Electromagnetic Shielding Effectiveness of Planar Materials. New York, NY, USA: ASTM, 1983.

[10] ASTM D5568-14. Standard Test Method for Measuring Relative Complex Permittivity and Relative Magnetic Permeability of Solid Materials at Microwave Frequencies Using Waveguide. West Conshohocken, PA, USA: ASTM International, 2014.

[11] Schelkunoff SA. Electromagnetic Waves. Princeton, NJ, USA: D. Van Nostrand, 1943.

[12] Shulz RB, Plantz VC, Brush DR. Shielding theory and practice. IEEE T Electromagn C 1988; 30: 187-201.

[13] Singh AP, Mishra M, Chandra A, Dhawan SK. Graphene oxide/ferrofluid/cement composites for electromagnetic interference shielding application. Nanotechnology 2011; 22: 5701.

[14] Saini P, Choudhary V, Singh BP, Mathur RB, Dhawan SK. Polyaniline-MWCNT nanocomposites for microwave absorption and EMI shielding. Mater Chem Phys 2009; 113: 919-926.

[15] Genç F, Turhan E, Kavas H, Topal U, Baykal A, Sözeri H. Magnetic and microwave absorption properties of NixZn0.9-xMn0.1Fe2O4 prepared by Boron addition. J Supercond Nov Magn 2015; 28: 1047-1050.

[16] Araz İ, Genç F. Microwave characterization of co-doped barium hexaferrite absorber material. J Supercond Nov Magn 2018; 31: 279-283.

[17] Wilson PF, Ma MT, Adams JW. Techniques for measuring the electromagnetic shielding effectiveness of materials. IEEE T Electromagn C 1988; 30: 239-259.

[18] Holloway CL, Hill DA, Ladbury J, Koepke G, Garzia R. Shielding effectiveness measurements of materials using nested reverberation chambers. IEEE T Electromagn C 2003; 45: 350-356.

[19] Baker J, Janezic MD, Riddle RF, Johnk RT, Kabos P, Holloway C, Geyer RG, Grosvenor CA. Measuring the Permittivity and Permeability of Lossy Materials: Solids, Liquids, Metals, Building Materials, and Negative-Index Materials. NIST Technical Note 1536, 2005.

[20] Stuchly SS, Matuszewski M. A combined total reflection transmission method in application to dielectric spectroscopy. IEEE T Instrum Meas 1978; 27: 285-288.

[21] Nicolson AM, Ross GF. Measurement of the intrinsic properties of materials by time-domain techniques. IEEE T Instrum Meas 1970; 19: 4.

[22] Weir WB. Automatic measurement of complex dielectric constant and permeability at microwave frequencies. P IEEE 1974; 62: 33-36.

[23] Nicolson AM. Broad-band microwave transmission characteristics from a single measurement of the transient response. IEEE T Instrum Meas 1968; 17: 395-402.

[24] Ligthardt LL. A fast computational technique for accurate permittivity determination using transmission line methods. IEEE T Microwave Theory Tech 1998; 42: 249-254.

[25] Baker J, Vanzura EJ, Kissick WA. Improved technique for determining complex permittivity with the transmission/reflection method. IEEE T Microw Theory Tech 1990; 8: 1096.

[26] Chen LF, Ong CK, Neo CP, Varadan VV, Varadan VK. Microwave Electronics Measurement and Materials Characterization. Chichester, UK: Wiley, 2004.

[27] Kaur T, Kumar S, Sharma J, Srivastava AK. Radiation losses in the microwave Ku band in magneto-electric nanocomposites. Beilstein J Naotechnol 2015; 6: 1700-1707.

[28] Handoko ME, Ivan S, Budi S, Anggoro BS, Mangasi AM, Randa Ö, Zulkarnain J, Kurniawan C, Sofyan N, Alaydrus M. Magnetic and microwave absorbing properties of $BaFe_{12-2x}Co_xZn_xO_{19}$ (x = 0.0; 0.2; 0.4; 0.6). Mater Res Express 2018; 5: 064003.